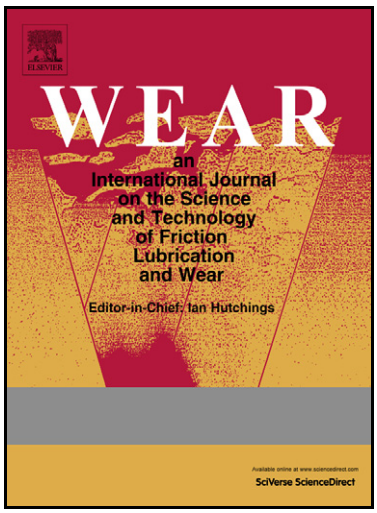

www.elsevier.com/locate/wear

Wear of nano-structured carbide-free bainitic steels under dry rolling-sliding conditions

A. Leiro, E. Vuorinen, K-G Sundin, B. Prakash, T. Sourmail, V Smanio, F.G. Caballero, C. Garcia-Mateo, Roberto Elvira

PII: S0043-1648(12)00407-3
DOI: http://dx.doi.org/10.1016/j.wear.2012.11.064
Reference: WEA100424

To appear in: *Wear*

Received date: 4 April 2012
Revised date: 10 October 2012
Accepted date: 21 November 2012

Cite this article as: A. Leiro, E. Vuorinen, K-G Sundin, B. Prakash, T. Sourmail, V Smanio, F.G. Caballero, C. Garcia-Mateo and Roberto Elvira, Wear of nano-structured carbide-free bainitic steels under dry rolling-sliding conditions, *Wear,* http://dx.doi.org/10.1016/j.wear.2012.11.064

Wear of nano-structured carbide-free bainitic steels under dry rolling-sliding conditions

*A. Leiro[1 *], E. Vuorinen[1], K-G Sundin[1], B. Prakash[1], T. Sourmail[2], V. Smanio[2], F.G. Caballero[3], C. Garcia-Mateo[3], Roberto Elvira[4]*

*Corresponding author's e-mail address: alejandro.leiro@ltu.se, Tel. +46(0)920 493109

1. Luleå University of Technology, Department of Engineering Sciences and Mathematics. Luleå 971-87, Sweden
2. ASCOMETAL-CREAS, 573-01 Hagondange Cedex, France
3. National Center for Metallurgical Research (CENIM-CSIC), E-28040 Madrid, Spain
4. Gerdau Sidenor I+D, E-48970 Spain

Abstract

Specially designed steels with carbon contents from 0.6 to 1.0 wt.% were isothermally transformed at very low temperatures, between 220 and 270°C, in order to obtain a nano-structured bainitic microstructure. It is shown that the wear resistance in dry rolling-sliding of these nano-structured steels is significantly superior to that of bainitic steels transformed at higher temperatures with similar hardness values**.** In addition to the highly refined microstructure, the transformation under strain to martensite (TRIP effect), contributes to the plasticity of the nano-scaled steels, increasing surface hardness during testing, thus reducing the wear rate.

Keywords: wear, rolling-sliding, steel, bainite, nanostructured materials.

1. Introduction

Development and design of nano-structured bainitic steels, as well as investigation of their tensile and toughness properties, has been the goal of a number of recent research studies [1-7]. These newly developed steels can reach ultimate tensile strengths of 2.5GPa, hardness of 600-670 HV and fracture toughness values ranging from 30 to 120 MPa.m$^{1/2}$.By careful design in the steel making process it is possible to obtain martensite transformation temperatures as low as 125°C . This allows isothermal treatments at very low temperatures. As a consequence, extremely fine microstructures (~30 nm lath thickness) are generated. The microstructure consists of laths of bainitic ferrite and retained austenite films in between. The main alloying element used is silicon, which added in amounts above 1,5% to the steel, will prevent cementite precipitation from austenite and make retained austenite a metastable phase at low temperatures. Other alloying elements are added in lower amounts to modify the onset temperature for martensite transformation, to refine the austenite grain size and consequently accelerate the transformation into bainite and to avoid transformations prior to bainite [8].

The aforementioned combination of mechanical properties is interesting from a wear point of view. Recently, studies have been made dealing with the sliding wear properties of this novel microstructure. Wang et al. [9] have investigated the pure-sliding wear properties. Their main findings included an improvement in wear resistance in relation with quenched and tempered bearing steel and the formation of ferritic nano-grains in the contact surface. Zhang et al. [10] obtained nano-structured bainite in the surface of a carburized low-C steel, matching the sliding wear performance of 20CrMnTi bearing steel in quench and tempered condition at loads of 240MPa. At 965 and1450 MPa the nano-scaled bainitic steel had a lower steady-state wear rate. Yang et al. [11] further reported that, for nano-scaled bainitic steels, the wear rate decreased proportionally with the austempering temperature when the transformation temperature varied between 200 and 260°C.

The investigation of the wear resistance of nano-scaled bainitic steels in different conditions is of great interest, given their potential use in engineering applications. One such case is rolling/sliding wear. Studies have been directed towards the investigation of carbide-free bainitic steels with isothermal transformation temperatures between 250 and 350°C. The results indicate that it is possible to obtain excellent wear performance by producing

steel with a bainitic ferrite microstructure without carbides. The first studies by Jin and Clayton [12, 13] reported that by obtaining a carbide-free bainitic microstructure, it was possible to match the wear properties of the best pearlitic rail steels in dry rolling/sliding conditions. Chang [14] reported that the ability to withstand large deformations is of great importance in the superior wear resistance exhibited carbide free bainitic steels. This suggests that the TRIP (transformation induced plasticity) effect can be beneficial in dry rolling/sliding wear since it is known to increase plasticity. Vuorinen et al. [15] found that it was possible to match the rolling-sliding wear performance of surface hardened steels by isothermal treatment of high-Si commercial steel with a carbide-free bainitic microstructure. Vuorinen et al. [16] and later Leiro et. al [17] studied the effect of retained austenite content on the rolling/sliding wear rate of high-Si steel with a carbide-free microstructure. It was found that at higher transformation temperatures and retained austenite content the wear rate increased.

In this work steels with carbon contents from 0.6 to 1.0% were austempered between 220 and 270°C in order to obtain a nano-bainitic microstructure. The wear characteristics of these specially designed steels have been studied under rolling/sliding conditions and compared with those of conventional steels having similar hardness values. Further, the wear mechanisms and surface features of these materials have also been investigated. Explanations are presented as to how the microstructural features are of key importance in the observed wear behavior.

2. Experimental

2.1 Material

Table 1 shows the chemical composition of the studied steels and the transformation temperatures used for each grade. The alloys contain sufficient C and Si to ensure low transformation temperatures and to avoid cementite precipitation from austenite respectively. The Cr and Mn content is enough to avoid other phase transformations prior to bainite. The design process has been extensively described in [8]. The temperature onset for martensite transformation has been determined experimentally by diferential dilatometry. The austenitization temperatures were: 950˚C for alloys 1C, 1CSi and 100Cr6 and 890˚C for alloys 09C and 06C.

In the following sections, the samples are referred to by the alloy abbreviation, followed by the transformation temperature in degreesCelsius. For example, sample 09C220 refers to alloy 09C treated at 220°C.

Transformation temperatures were selected in order to produce microstructures with different mechanical properties. The transformation times were varied in each case to achieve complete transformation into bainite, according to dilatometry analyses. In order to compare the current steels, 100Cr6 steel transformed at 250 and 300°C was used as reference material for the wear tests. The reference steel presented a lower-bainitic microstructure and contained between 1-3% of globular carbides.

2.2 Microstructural analysis

A Jeol JSM 6460 scanning electron microscope (SEM) was used to investigate the microstructures. SEM micrographs were taken both before and after the wear tests to examine the microstructure. Prior to the examination, classical metallographic sample preparation was performed. Etching was done with 2% Nital for 5-10 seconds. After completion of the wear tests, the worn surfaces of test disc specimens were studied by using SEM without disturbing the actual surface. Finally, cross-sections of the studied discs were cut in order to study the microstructural evolution of the sub-surface region.

Retained austenite measurements prior to wear tests were carried out using X-ray diffraction analysis. An electropolished surface was used in order to avoid any impact of the grinding/polishing operations [18]. The average bainite lath thickness was measured on SEM micrographs, carrying at least 100 measurements in all cases, and accounting for stereological effects [19]

2.3 Wear tests

Rolling/sliding tests were done using a UTM 2000 twin-disc machine. The specimens were cylindrical discs of 45 mm diameter and 10 mm thickness. The resulting contact geometry is, therefore, a line contact. The maximum Hertzian contact pressure was 1400 MPa (approximately) at the beginning of the test since the full width of the sample was not in contact, mainly due to misalignment and geometric/dimensional tolerances. However, the contact width increased during the test as a consequence of wear, and the contact pressure decreased to a value of approximately 400 MPa once the full contact was established. The material pairs were self-mated and tested in ambient conditions (25 °C, 23% humidity) without lubrication. The samples were tested for a total duration of five hours, the rotational speed was approximately 100 rpm and the slip was kept at 5% in all tests. Further details of the testing procedure can be found in [17].

3. Results

3.1 Microstructure

Figure 1 presents a micrograph of the observed microstructures for sample 09C transformed at 220 and 250°C. The materials exhibited bainitic microstructures consisting of ferrite laths separated by thin films of retained austenite. The laths were nano-scaled, with an average bainite lath thickness between 32 and 60 nm.

In Table 2 the lath thickness and austenite content for all alloys are presented. As expected [20] lath thickness does not change significantly between the 1C and 09C samples, since carbon content is of utmost importance for bainite lath thickness. As can be seen for sample 06C the lath thickness increased considerably. The retained austenite content was highest in the alloy with 1%C and 2.9% Si and lowest in the 06C 250 alloy. Temperature did not affect the retained austenite content in the three 09C samples. This is because the transformation times were changed in order to achieve full transformation.

3.2 Wear

In Figure 2, the rolling-sliding specific wear rates are presented. The specific wear rate is an expression of the volume loss divided by the load and sliding distance. The volume loss was calculated from the sum of the mass loss of both discs involved in the test, i.e. the wear rate of the tribo-pair. For comparison, results previously published by Leiro et al. [17] on carbide-free bainitic steels (60SiCr7spring- steel austempered at 250 and 300˚C respectively) have been included in the plot. These results were obtained under identical conditions as in the current tests. The nano-structured steels show considerably higher wear resistance in comparison to the reference steels. The wear rates of the nano-structured steels are approximately half of that of the reference steels at 600 HV.

3.3 Worn Surface Observations

In order to identify the wear mechanisms, SEM observations of the worn surfaces and of the cross-section of selected samples were done. In Figure 3, SEM images of the worn surfaces of samples 1CSi250 and 100Cr6 250 are shown. The main types of damage observed are surface cracking, indentations and accumulation of oxidized wear debris.

The indentation depths are not the same in all samples as can be observed when comparing Figure 3 (a) and (b). These indentations can be caused by two different mechanisms. They can be the result of flakes of material that were removed from the surface. It is also possible that wear debris accumulated in the surface agglomerated in such a way that when it came into the contact, it caused plastic deformation of the surface as has been observed previously [17].

3.4 Analysis of disc cross-sections

In Figure 4, micrographs of sections through disc specimens 09C220 and 1CSi250 are presented. The porosity observed is a result of the manufacturing process. In this study, the disc specimens used were manufactured from "experimental casts" in which the plastic deformation of the casting during the steel making process was limited. Therefore, porosity could not be completely removed. The micrographs present the typical damage modes observed in all the disc test specimens. These include deformation of the microstructure in the direction of sliding and delamination or "flaking". As can be observed in Figure 4, the deformed microstructure is oriented in the direction of sliding which has also been previously observed for pearlitic rail steels. In the case of pearlitic steels, the alignment and refinement of the cementite plates, along with the deformation of the surface are considered to be a reason for their successful performance in rolling-sliding wear [21]. In carbide-free steels there is no cementite, however, there is high-carbon retained austenite, which can transform to martensite under strain. This transformation, in addition to the deformation hardening, causes the hardness to increase considerably at the contact surface, as has been reported in the past by Leiro et al. [17].

4. Discussion

Due to the slip at which the tests were performed (5%), the high adhesive forces present are responsible for the generation of wear debris at the beginning of the tests. The debris gets oxidized due to frictional heating and can be entrapped into the contact. It can also be embedded and/or cause indentation of disc surfaces. The presence of oxidized wear debris can also lead to some abrading action. However, the contact area is very small (line contact) and large abrasion marks cannot be generated.

The surface cracks observed in Figure 3 were identified as delaminating flakes in the disc cross-sections (Figure 4), and this is in accordance with previous findings [17]. This damage mechanism has been observed in all the studied specimens and, according to the worn surface observations (Figure 3), it appears to be the main mechanism of material removal in all cases, including the reference steel (100Cr6). Delamination is caused by rolling contact fatigue (RCF). Cracks that grow due to RCF, will either nucleate at the surface or below the surface depending on the friction levels. Once a crack is nucleated at the surface, it will tend to grow into the bulk of the material initially, afterwards parallel to the surface and finally back towards the surface until the whole flake is removed [22].

Adhesive forces play an important role under the current conditions. While no adhesive damage was observed by the SEM study of the worn surfaces, the friction levels ranged between 0.55 and 0.65. This suggests that significant adhesive forces exist in the contact. In addition, the deformed microstructure observed in Figure 4 is direct evidence of the presence of high adhesion in the contact. In Figure 5 (a), a crack growing from the base of a deformed asperity can be seen, indicating that sliding aids in the crack nucleation process. Furthermore, once cracks have grown to a certain extent, the sliding forces can generate secondary cracking at the base of the delaminating flake (Figure 5 (b)), accelerating material removal. The orientation of the bainitic laths in the direction of sliding also creates preferential paths at the lath interfaces for the RCF cracks to grow along. Therefore, even though RCF is the main mechanism of crack growth, an important effect of sliding forces is clearly present in the studied samples. It is important to note that the hardness of the material is very important in resisting the action of sliding forces. Therefore, it is understandable that samples exhibit lower wear rates as the hardness increases (Figure 2).

Among the 09C grade steel, it was observed (Figure 3) that the hardness increased and the wear rate decreased with lowering of the transformation temperature. However, all three 09C grades (220, 250 and 270) present similar amount of retained austenite and bainite lath thickness. Therefore, the observed change in hardness can be attributed to the dislocation density, which has been shown to increase in nanostructured steels with lowering the transformation temperature [23]. A higher amount of dislocations will further resist plastic deformation, increasing tensile strength and hardness.

The toughness of the material or how much deformation the material can withstand without breaking is another key property in wear. This will determine how easily asperities being deformed in the contact can break. Yang et al. [11] reported that nearly all the retained austenite in the worn surface of nano-structured bainitic steel subjected to sliding wear will transform into martensite. This shows that the TRIP effect is present during deformation under sliding wear for this type of steel. The TRIP effect can be beneficial since it can increase the ductility of the steel [24]. This will in turn increase toughness, and also wear resistance. An example of the effect of retained austenite on the wear properties can be seen when comparing samples 1C250 and 1CSi250. Even though the hardness of sample 1CSi250 is slightly lower, due to a higher amount of retained austenite, its average wear rate is 20% lower (Figure 3). Since the transformation temperature and average bainite lath thickness is similar in both samples (Table 2), the observed wear behavior can be attributed to the higher retained austenite content, and higher plasticity exhibited by the 1CSi250 sample.

Sample 06C250 presented considerably lower hardness than the other steels. However, its wear rate was of the same magnitude as 1C and 09C grades transformed above 250°C. Despite having the lowest retained austenite content, this sample has lower hardness than all other samples, which is expected due to its lower carbon content. A lower amount of carbon means that the steel can present higher ductility and toughness and lower hardness. Figure 6 presents the specific wear rate of the studied alloys as a function of surface hardness after wear. As can be seen, the trend is that at higher final surface hardness, the wear rate is lower, which is in accordance with previous discussions. This is further evidence that higher toughness and hardening during wear can also contribute to decreasing wear in nano-bainitic steels.

It could be seen in Figure 3 that the results present considerable scatter in some cases. Wear can introduce local heating, chemical reactions and other unforeseeable changes in the contact surface. In addition, the deformed material is often not removed from the surface after one cycle, and its mechanical properties undergo changes during subsequent cycles. All these factors can account for the scatter observed in the wear results.

Since hardness affects the stress needed to deform the asperities in the contact, it is a determining factor in decreasing wear. The hardening ability of the material is equally important, since it will affect the final hardness the surface can achieve during wear. Part of the hardening will be achieved by deformation. The transformation of retained austenite into martensite under strain will also be responsible for a certain amount of hardening. As can be seen in Figure 6 as the hardness decreases, the wear rate of the nano-scaled alloys seems to reach a constant value. This shows that not only hardening is affecting wear. Other important factors can include toughness, or the amount of deformation the material can withstand before fracture. In the nano-structured steels with lower initial or final hardness, increased toughness is responsible for the wear rate exhibited.

5. Conclusions

In this work, steels with carbon contents from 0.6 to 1.0 wt.% were transformed between 220 and 270°C to produce nano-structured bainite with a lath thickness between 32 and 60 nm.

These nano-structured steels exhibit significantly lower specific wear rates when compared to the reference 100Cr6 with lower bainite microstructure and other conventional carbide-free bainitic steels, even at the same hardness levels. At hardness values of approximately 600 HV, the wear rate was reduced by half.

Rolling contact fatigue (RCF) was determined to be the main mechanism of material removal. Adhesive forces present an important factor in creating crack initiation sites for RCF cracks. The alignment of the microstructure along the sliding direction is also a determining factor in the RCF crack growth since it creates preferential paths for cracks to grow along. Adhesion will also aid in flake removal.

Toughness has been shown to improve wear resistance. The TRIP effect can be beneficial towards wear if it increases the toughness of the material i.e. if the stability of the retained austenite is high.

Since hardness affects the stress needed to deform the material in the rolling/sliding contact, it is a determining factor in decreasing material loss. The hardening ability of the material (deformation + transformation) is equally important, since it will affect the final hardness the surface can achieve during wear.

6. Acknowledgements

The authors gratefully acknowledge the financial support from the European Commission Research Fund for Coal and Steel for this research under the contract number RFSR-CT-2008-00022. F.G. Caballero and C. Garcia-Mateo also acknowledge the Spanish Ministry of Science and Innovation Plan Nacional de I+D+I (2008-2011) for its financial support under the contract MAT2010 - 15330.

7. References

1. F.G. Caballero, H.K.D.H. Bhadeshia, Very strong bainite, Curr. Opin. Solid St. M. 8 (2004) 251-257.
2. S. K. Putatunda, A. V. Singara, R. Tackett, G. Lawes, Development of a high strength high toughness ausferritic Steel, Mater. Sci. Eng. A Struct. Mater. 513–514 (2009) 329–339.
3. C. Garcia-Mateo, F. G. Caballero, H.K.D.H. Bhadeshia, Development of hard bainite, ISIJ Int. 43 (2003) 1238–1243.
4. C. Garcia-Mateo, F. G. Caballero, H.K.D.H. Bhadeshia, Acceleration of low-temperature bainite, ISIJ Int. 43 (2003) 1821–1825
5. C. Garcia-Mateo, F. G. Caballero, Ultra-high-strength bainitic steels, ISIJ Int. 45 (2005) 1736–1740
6. C. Garcia-Mateo, F. G. Caballero, H.K.D.H. Bhadeshia, Low temperature bainite, J Phys. IV. 112 (2003) 285-288
7. F. G. Caballero, C. García-Mateo, C. Capdevila, C. García de Andrés, Advanced Ultrahigh Strength Bainitic Steels, Mater. Manuf. Process. 22 (2007) 502-506
8. C. Garcia-Mateo, F.G. Caballero, Design of carbide-free low-temperature ultra high strength bainitic steels, Int. J. Mater. Res. 98 (2007) 137-143
9. T.S. Wang, J. Yang, C.J. Shang, X.Y. Li, B. Lv, M. Zhang, F.C. Zhang, Sliding friction surface microstructure and wear resistance of 9SiCr steel with low-temperature austempering treatment, Surf. Coat. Tech. 202 (2008) 4036–4040
10. P. Zhang, F.C. Zhang, Z.G. Yan, T.S. Wang, L.H. Qian, Wear property of low-temperature bainite in the surface layer of a carburized low carbon steel. Wear 271 (2011) 697-704
11. J. Yang, T.S. Wang, B. Zhang, F.C. Zhang, Wear (2012), Sliding wear resistance and worn surface microstructure of nanostructured bainitic steel, doi:10.1016/j.wear.2012.02.008
12. N. Jin, P. Clayton, Effect of microstructure on rolling/sliding wear of low carbon bainitic steels, Wear. 202 (1997) 202–207

13. P.Clayton, N. Jin, Unlubricated sliding and rolling/sliding wear behavior of continuously cooled, low/medium carbon bainitic steels, Wear. 200 (1996) 74-82

14. L.C. Chang, The rolling/sliding wear performance of high silicon carbide-free bainitic steels, Wear. 258 (2005) 730-743

15. E. Vuorinen, D. Pino, J. Lundmark, B. Prakash, Wear characteristic of surface hardened ausferritic Si-steel, J. Iron Steel Res. Int. 14 (2007) 245–248

16. E. Vuorinen, L. Wang, S. Stanojevic, B. Prakash, Influence of retained austenite on rolling-sliding wear resistance of austempered silicon alloyed steel, Proceedings of Hot Sheet Metal Forming of High-Performance Steel, 2nd International Conference. Sweden (2009)

17. A. Leiro, A. Kankanala, E. Vuorinen, B. Prakash, Tribological behaviour of carbide-free bainitic steel under dry rolling/sliding conditions, Wear 273 (2011) 2-8

18. J. Dyson and B. Holmes, Effect of alloying additions on the lattice parameter of austenite, J. Iron Steel Inst. 208 (1970) 469-474

19. L.C. Chang, H. Bhadeshia, Austenite films in bainitic microstructures, Mat. Sci. Tech. 11 (1995) 874-882

20. B. Singh, H.K.D.H. Bhadeshia, Estimation of bainite plate-thickness in low-alloy steels, Mater Sci Eng A. 245 (1998) 72-79

21. J. Perez-Unzueta, J. H. Beynon, Microstructure and wear resistance of rail steels. Wear, 162-164 (1993) 173-182

22. Van Beek, Advanced Engineering Design, first ed., www.engineeringabc.com, Netherlands, 2009, ISBN 9-08104-061-8.

23. C. Garcia-Mateo, F.G. Caballero, H.K.D.H Bhadeshia, Mechanical properties of low-temperature bainite, Mat. Sci. For. 500-501 (2005) 495-502

24. H.K.D.H. Bhadeshia, TRIP-assisted steels?, ISIJ Inter., 42 (9) (2002) 1059-1060

Figure 1. Typical microstructure as observed in a scanning electron microscope (SEM) a) 09C 220 and b) 09C 250

Figure 2. Specific wear rate vs. hardness plot of studied alloys and data from Leiro et al. [17] of tests done at the same conditions for other carbide-free bainitic steels.

Figure 3. Worn surface SEM micrographs of steels tested under dry rolling/sliding. Notice surface cracking, indentation and agglomeration of debris in the surface. The upwards arrows indicate the sliding direction.

Figure 4. Longitudinal section micrographs showing surface delamination and orientation of the microstructure with the sliding direction. Etched with nital 2%, 5 seconds. The white arrows indicate the direction of sliding.

Figure 5. Cross section micrographs of 09C 270 showing a) early and b) late flaking.

Figure 6 Specific wear rate as a function of final surface hardness for the studied alloys

Table 1. Composition, Ms Temperature, transformation temperature and abbreviation of the tested alloys

Alloy	C	Si	Mn	Cr	Ms Temperature (°C)	Transformation Temperature (°C) (time)
1C	0.99	1.50	0.76	0.46	130	250 (16h)
1CSi	0.98	2.90	0.77	0.45	160	250 (16h)
09C	0.9	1.65	0.79	0.48	160	220 (22h), 250 (16h), 270 (7h)
06C	0.68	1.60	1.25	1.50	220	250 (12h)
100Cr6	1.00	0.3	0.3	1.5	220	250 (1.5h), 300 (1h)

Table 2. Microstructural parameters and mechanical properties of studied alloys.

Alloy	Bainite lath thickness (nm)	Retained Austenite Fraction (%)	Hardness (HV0.5)
1C 250	38	20	660
1CSi 250	39	33	630
09C 220	32	22	693
09C 250	38	18	640
09C 270	36	24	621
06C 250	60	12	589
100Cr6 250	-	-	712

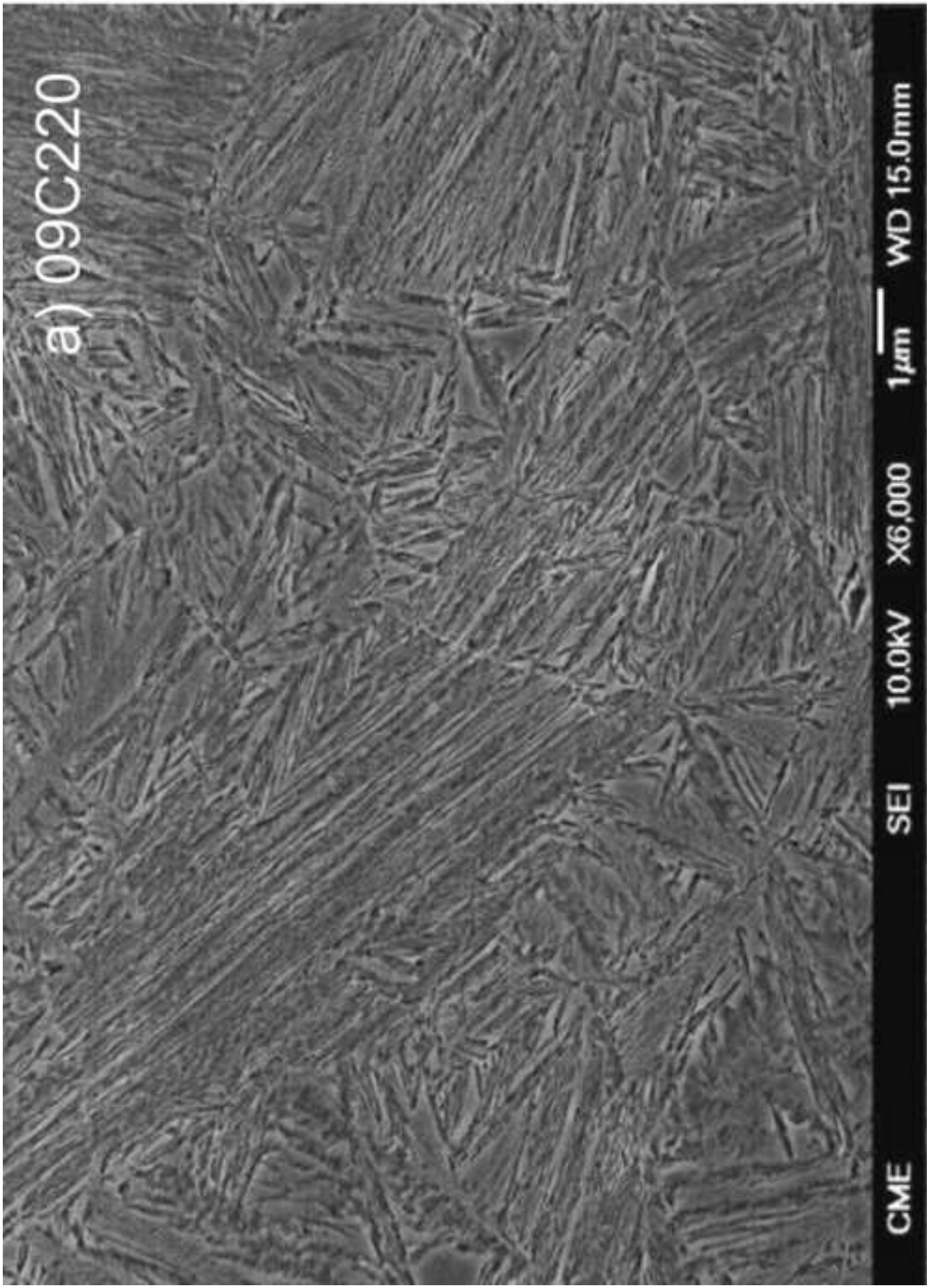

Figure 1a

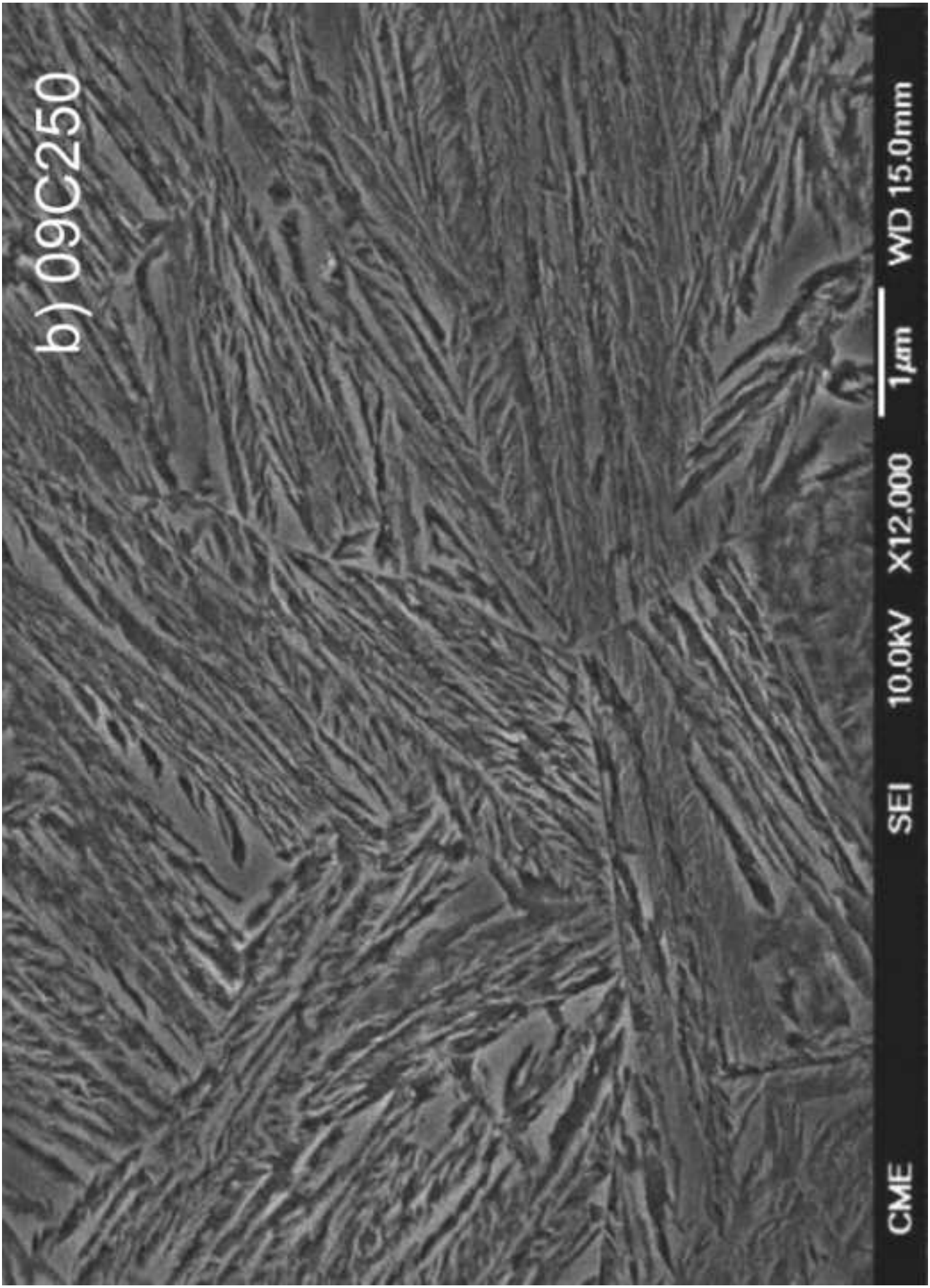

Figure 1b

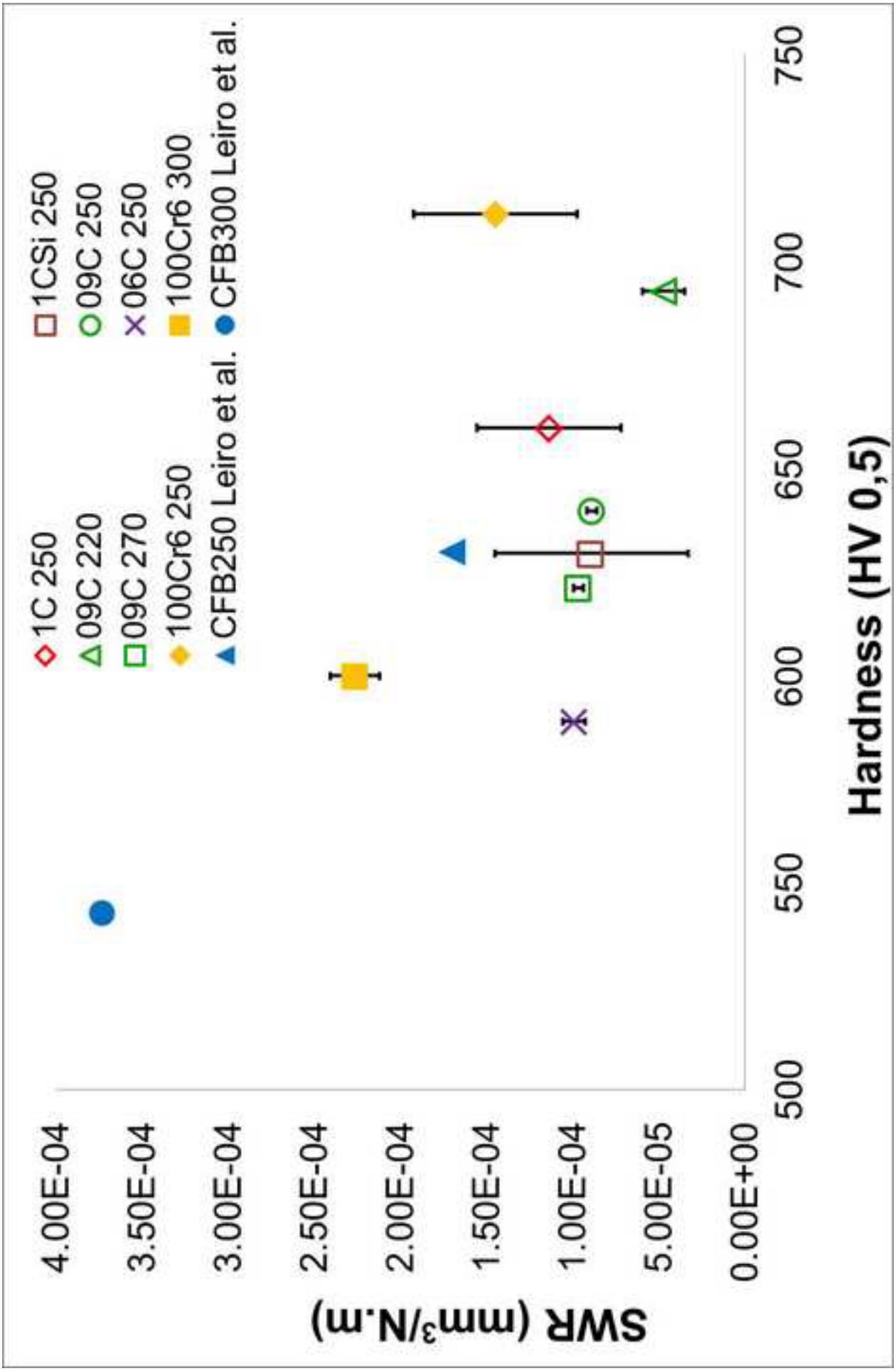
1C 250
09C 220
09C 270
100Cr6 250
CFB250 Leiro et al.
1CSi 250
09C 250
06C 250
100Cr6 300
CFB300 Leiro et al.
SWR (mm³/N.m)
4.00E-04
3.50E-04
3.00E-04
2.50E-04
2.00E-04
1.50E-04
1.00E-04
5.00E-05
0.00E+00
500
550
600
650
700
750
Hardness (HV 0,5)

Figure 2

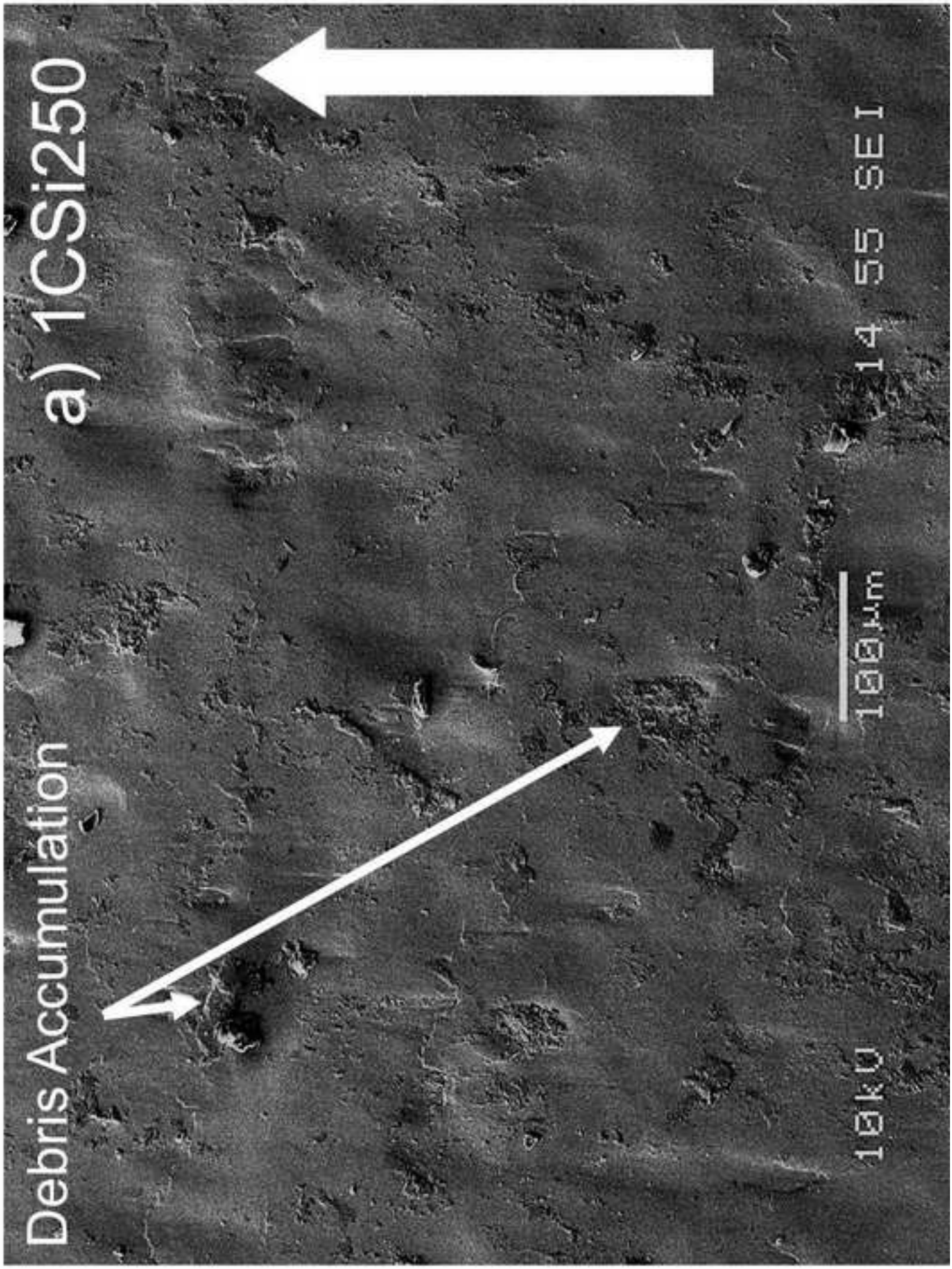

Figure 3a

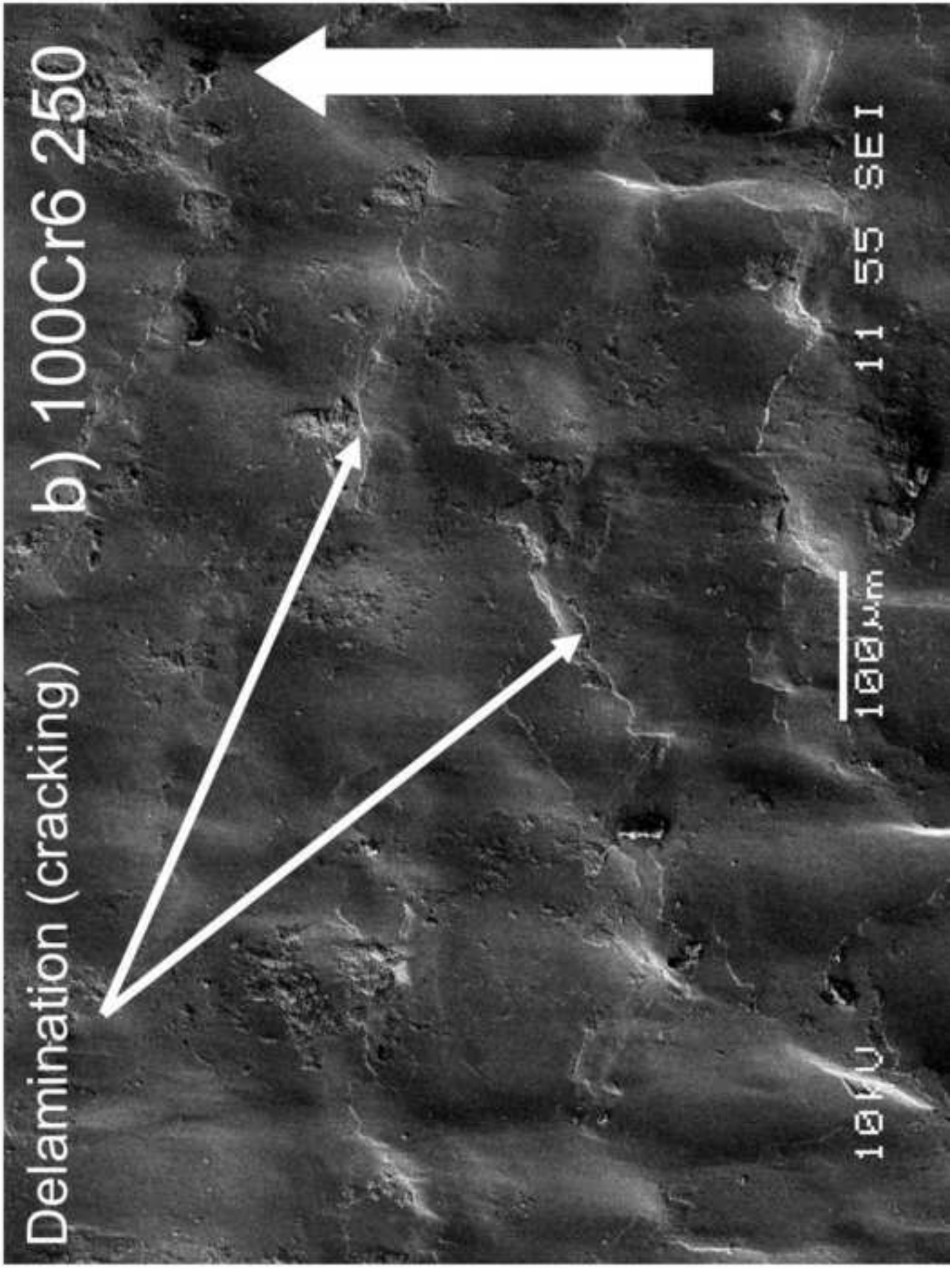

Figure 3b

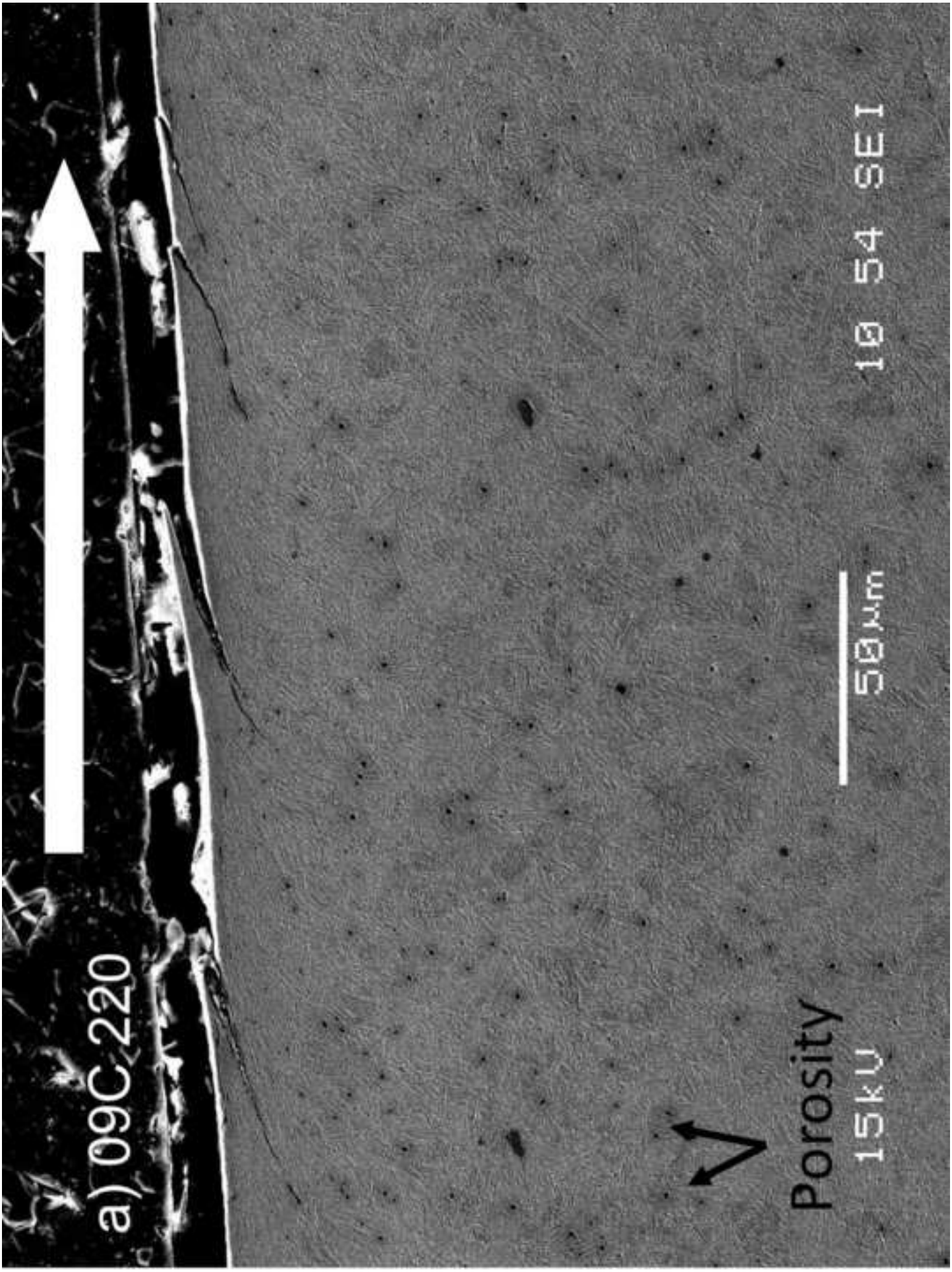

Figure 4a

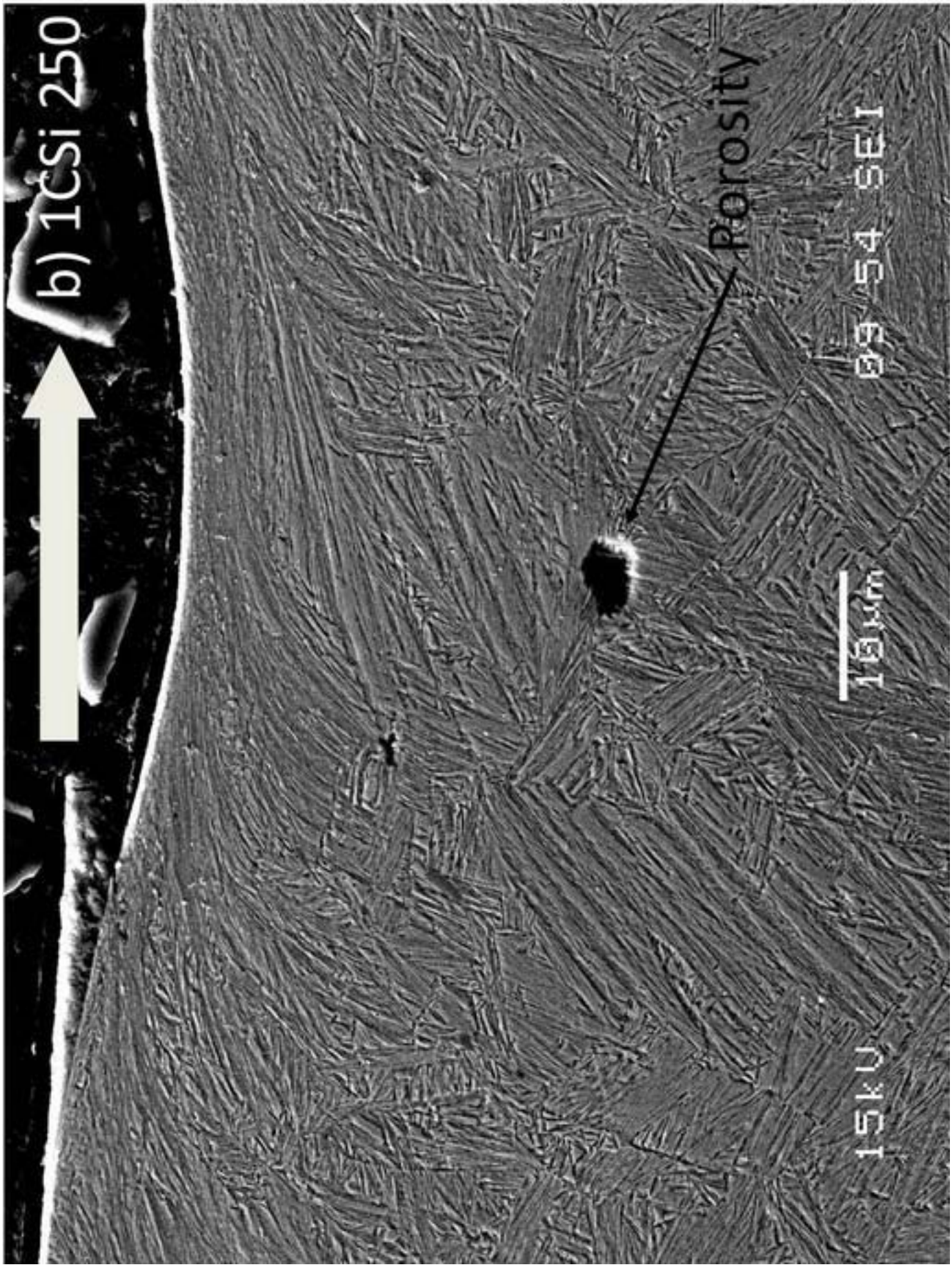

Figure 4b

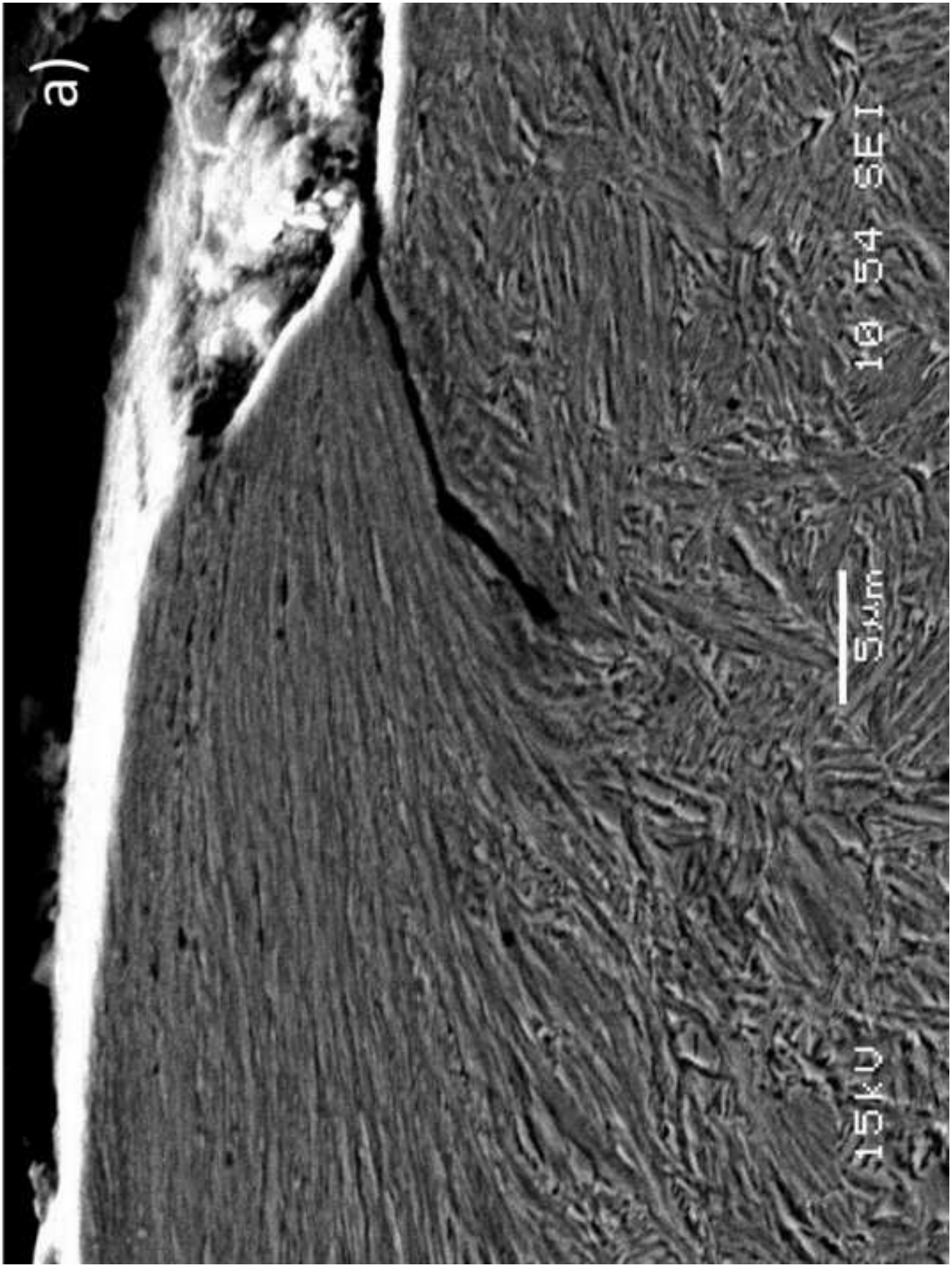

Figure 5a

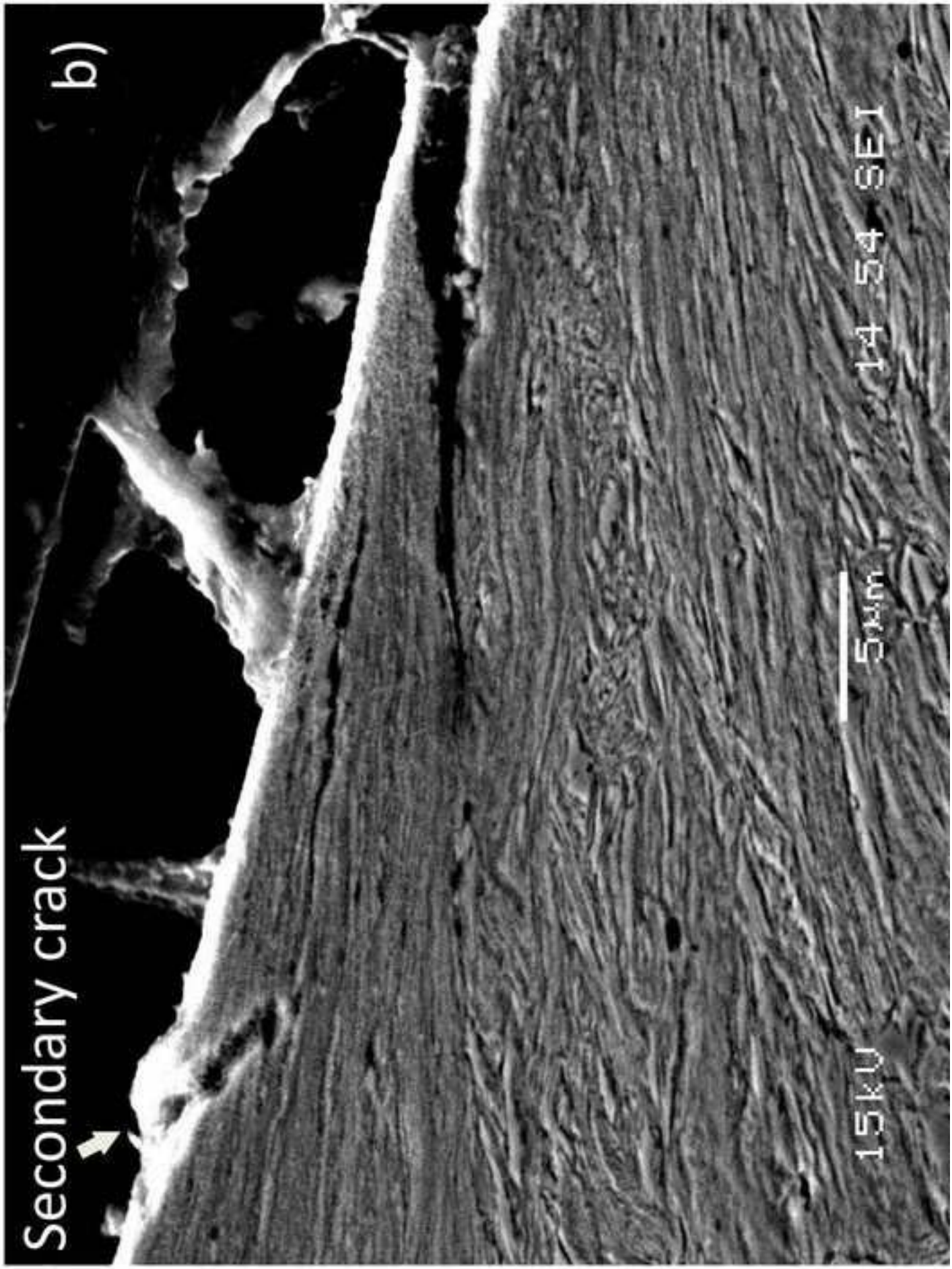

Figure 5b

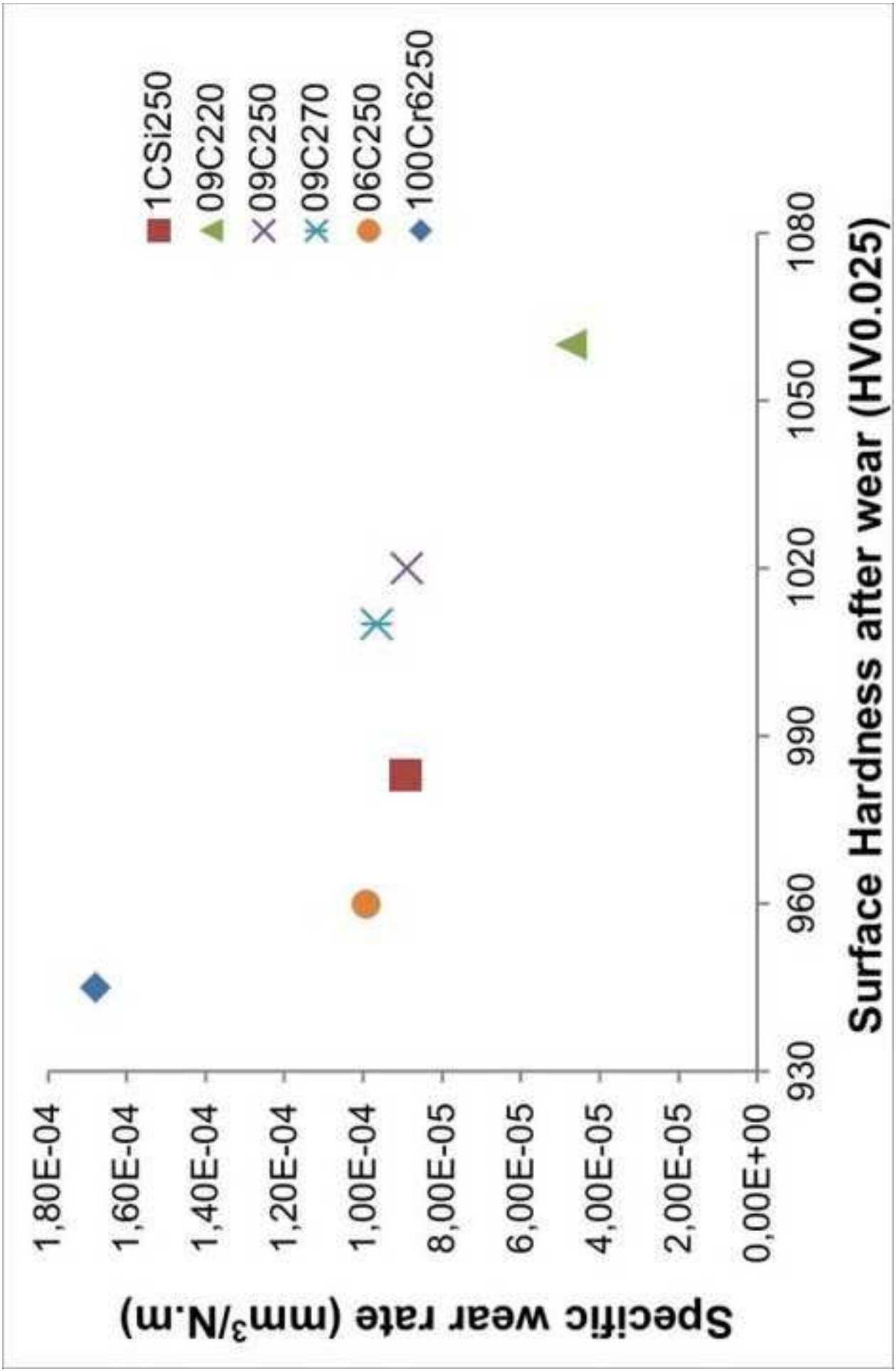
1CSi250
09C220
09C250
09C270
06C250
100Cr6250
Specific wear rate (mm3/N.m)
1,80E-04
1,60E-04
1,40E-04
1,20E-04
1,00E-04
8,00E-05
6,00E-05
4,00E-05
2,00E-05
0,00E+00
930
960
990
1020
1050
1080
Surface Hardness after wear (HV0.025)

Figure 6